DMD Fast Forward. Published on July 12, 2013 as doi:10.1124/dmd.113.052514

DMD #52514

In vitro Investigation of Amyloid-beta Hepatobiliary Disposition in Sandwich Cultured Primary Rat Hepatocytes

Loqman A. Mohamed and Amal Kaddoumi

Department of Basic Pharmaceutical Science, College of Pharmacy, University of Louisiana at Monroe. 1800 Bienville Dr., Monroe, LA 71201

DMD Fast Forward. Published on July 12, 2013 as DOI: 10.1124/dmd.113.052514
This article has not been copyedited and formatted. The final version may differ from this version.

Running Title: $A\beta_{40}$ biliary excretion in SCHs.

To whom correspondence should be addressed: Dr. Amal Kaddoumi, College of Pharmacy, University of Louisiana at Monroe, 1800 Bienville Dr., Monroe, LA 71201. Phone: (318) 342-1460; Fax: (318) 342-1737; E-mail: kaddoumi@ulm.edu

Number of text pages: 233

Number of tables: 0

Number of figures: 9

Number of references: 52

Number of words in the abstract: 240

Number of words in the introduction: 757

Number of words in the discussion: 1488

Abbreviations

AD, Alzheimer's disease; Aβ, amyloid-beta; BEI%, biliary excretion index; BBB, blood-brain barrier; BSA, bovine serum albumin; BCA, bicinchoninic acid; Cl_{bile}, biliary clearance; CDFDA, 5-(and-6)-carboxy-2',7'-dichlorofluorescein diacetate; CDF, 5-(and-6)-carboxy-2',7'-dichlorofluorescein; DMEM, Dulbecco's modified Eagle's medium; ECE, endothelin-converting enzyme-1; EGTA, ethylene glycol tetraacetic acid; FBS, fetal bovine serum; HFP, 1,1,1,3,3,3-Hexafluoro-2- propanol; HBSS, Hanks Balanced Salt Solution; IDE, insulin-degrading enzyme; LRP1, low density lipoprotein-receptor related protein-1; MRP2, multidrug resistance-associated protein 2; NEP, neprilysin; P-gp, P-glycoprotein; Rh123, rhodamine 123; RAGE, receptor for advanced glycation end products; RAP, receptor-associated proteins; sLRP, soluble low-density lipoprotein receptor-related protein; SCHs, sandwich cultured primary rat hepatocytes; TCA, trichloroacetic acid.

DMD Fast Forward. Published on July 12, 2013 as DOI: 10.1124/dmd.113.052514
This article has not been copyedited and formatted. The final version may differ from this version.

Abstract

Failure in amyloid beta (Aβ) systemic clearance across the liver has been suggested to play a role in Aβ brain accumulation and thus contributes largely to Alzheimer's disease (AD) pathology. The purpose of this study was to in vitro characterize the transport mechanisms of $A\beta_{40}$ across the liver using sandwich cultured primary rat hepatocytes (SCHs) and determine its biliary clearance (Cl_{bile}) and biliary excretion index (BEI%). ^{125}I-$A\beta_{40}$ BEI% was time dependent and reached steady state at 30min with an average value of 29.8% and Cl_{bile} of 1.47ml/min/kg. The role of low density lipoprotein-receptor related protein-1 (LRP1) in mediating the basolateral uptake of ^{125}I-$A\beta_{40}$ in SCHs was assessed using receptor-associated protein (RAP, 2μM). Significant reduction in ^{125}I-$A\beta_{40}$ BEI% and Cl_{bile} with RAP was observed, demonstrating a major contribution of LRP1 in mediating hepatic uptake of intact ^{125}I-$A\beta_{40}$ via transcytosis. Furthermore, activity studies suggested lower role of receptor for advanced glycation end products (RAGE) in ^{125}I-$A\beta_{40}$ hepatic uptake. Verapamil (50μM) and valspodar (20μM) significantly reduced ^{125}I-$A\beta_{40}$ BEI% indicating a role for P-glycoprotein (P-gp) in the biliary excretion of ^{125}I-$A\beta_{40}$ in SCHs. LRP1 and P-gp mediated ^{125}I-$A\beta_{40}$ biliary excretion was inducible and increased BEI% by 26% following rifampicin pretreatment. In conclusion, our findings demonstrated that beside LRP1, P-gp and to a lesser extent RAGE are involved in ^{125}I-$A\beta_{40}$ hepatobiliary disposition, and support that enhancement of Aβ hepatic clearance via LRP1 and P-gp induction as a novel therapeutic approach for AD prevention and treatment.

DMD Fast Forward. Published on July 12, 2013 as DOI: 10.1124/dmd.113.052514
This article has not been copyedited and formatted. The final version may differ from this version.

Introduction

Alzheimer's disease (AD) is a complex neurodegenerative disease and the most common cause of dementia (Sagare et al., 2012). AD is characterized by specific neuropathological lesions including progressive deposition of intracellular neurotoxic form of the amyloid-beta (Aβ) peptides, Aβ40 and Aβ42, and extracellular Aβ as senile plaques throughout the brain (Makarova et al., 2004). It is suggested that elevated levels of brain Aβ monomers resulted in formation of neurotoxic Aβ oligomers which contribute largely to the pathogenesis of this disease (Zhao et al., 2012). Aβ is produced by enzymatic cleavage, mediated by β- and γ-secretases, of the transmembrane protein amyloid precursor protein (APP) (Cam and Bu, 2006). The high levels of Aβ observed in brain of AD patients are mainly due to overproduction of Aβ and/or failure of its clearance from the brain (Sommer, 2002). As a peptide, $A\beta_{40}$ has poor passive membrane permeability and it depends on a transport system to pass through endothelial cells of blood-brain barrier (BBB) (Banks et al., 2003). Low density lipoprotein receptor related protein-1 (LRP1) is the major receptor that mediates removal of Aβ across the BBB in its free form (Deane et al., 2004), or bound to chaperon molecules such as apolipoprotein E (ApoE). P-glycoprotein (P-gp), expressed on the luminal side of the BBB, mediates the efflux of Aβ into the peripheral circulation (Cirrito et al., 2005). It has been reported that the expression of LRP1 and P-gp at the BBB is decreased and expression of receptor of advanced glycation end product (RAGE), which influx circulating Aβ into the brain across the BBB, is increased in AD patients, which favors Aβ accumulation inside the brain (Castellano et al., 2012; Deane et al., 2003; Deane et al., 2012; Donahue et al., 2006; Sagare et al., 2007). In addition to role of Aβ transport proteins, several Aβ degrading enzymes have been shown to significantly contribute to Aβ clearance. Numerous *in vitro* and *in vivo* studies support the physiological role of insulin-

DMD Fast Forward. Published on July 12, 2013 as DOI: 10.1124/dmd.113.052514
This article has not been copyedited and formatted. The final version may differ from this version.

degrading enzyme (IDE), neprilysin (NEP), endothelin-converting enzyme-1 (ECE-1) and ECE-2, among others, in Aβ degradation (Eckman and Eckman, 2005; Saido and Leissring, 2012). Plasma Aβ, including Aβ that is effluxed from the brain, undergo rapid clearance mainly through the liver in its free or plasma lipoprotein-bound form (Marques et al., 2009; Tamaki et al., 2006). Recently, several reports have shown that endogenous soluble circulating low-density lipoprotein receptor-related protein (sLRP) plays an important role in clearance of systemic Aβ "sink activity" and maintenance of Aβ brain homeostasis (Quinn et al., 1997; Sagare et al., 2007). sLRP normally binds 70-90% of circulating plasma Aβ and forms complexes that are unable to enter the brain across the BBB and favor its elimination mainly through the liver (Deane et al., 2008; Sagare et al., 2011); however, in AD, sLRP1 is mostly oxidized which prevent its binding to circulating $A\beta_{40}$ causing sharp increase in free $A\beta_{40}$ plasma levels (Sagare et al., 2011).

LRP1 is expressed abundantly in the liver, mainly in hepatocytes, and is considered the major receptor that clears Aβ from the general circulation (Tamaki et al., 2006). Receptor-associated protein (RAP) has shown to inhibit $A\beta_{40}$ liver uptake in rats by 48%, indicating the role of LRP1 in mediating the hepatic uptake of ^{125}I-$A\beta_{40}$ from the circulation (Tamaki et al., 2006). In another study, portal infusion of insulin increased the expression of hepatic LRP1 at the cell membrane in a time dependent manner, and induced the apparent hepatic uptake of $A\beta_{40}$ in a concentration dependent manner (Tamaki et al., 2007). Several studies have demonstrated the involvement of liver as a main pathway in the clearance of Aβ from the peripheral circulation and have shown that faulty clearance of plasma free Aβ contributes largely to AD (Ghiso et al., 2004; Sagare et al., 2007; Sutcliffe et al., 2011). These studies, however, focused on LRP1 contribution to the hepatic clearance of Aβ. Although LRP1 was determined to be the major pathway for Aβ systemic clearance, other mechanisms of transport in the liver that play role in

Aβ hepatic clearance need further investigation. Hence, in the current study we aimed to characterize the mechanism of $A\beta_{40}$ hepatic uptake as well as biliary excretion and to address the role of P-gp, LRP1 and RAGE in this process using sandwich cultured primary rat hepatocytes (SCHs), which impart the advantage of studying the vectorial transport of substrates. Since P-gp and RAGE are expressed in the brain and they contribute to Aβ brain homeostasis, we hypothesized that both of these transport proteins, beside LRP1, mediate the hepatic uptake and biliary elimination of $A\beta_{40}$.

DMD Fast Forward. Published on July 12, 2013 as DOI: 10.1124/dmd.113.052514
This article has not been copyedited and formatted. The final version may differ from this version.

Materials and Methods

Materials. Collagenase (type I, class I), rat tail collagen (type I), Dulbecco's modified Eagle's medium (DMEM), and insulin were purchased from Invitrogen (Carlsbad, CA). Rifampicin, caffeine, 1,1,1,3,3,3-Hexafluoro-2- propanol (HFP), rhodamine123 (Rh123), dexamethasone, bovine serum albumin (BSA), 10X DMEM, soybean trypsin inhibitor, and fetal bovine serum (FBS) were purchased from Sigma-Aldrich (St. Louis, MO). Synthetic monoiodinated and nonoxidized ^{125}I-Aβ_{40} (human, 2200 Ci/mmol) was purchased from PerkinElmer (Boston, MA). [^{14}C] Salicylic acid and [^{3}H] taurocholate were obtained from American Radiolaeled Chemicals (St. Louis, MO). ITS culture supplement (10µg/ml insulin, 10µg/ml transferrin, 10ng/ml selenous acid) was obtained from BD Biosciences (San Jose, CA). RAP was purchased from Oxford Biomedical Research (Oxford, MI). Valspodar was obtained from XenoTech (Lenexa, KS). The reagents and supplements required for western blotting were purchased from Bio-Rad (Hercules, CA). For western blot, the mouse monoclonal antibody C-219 against P-gp was obtained from Covance Research Products (Dedham, MA); mouse monoclonal antibody against light chain LRP1 was obtained from Calbiochem (Gibbstown, NJ); mouse monoclonal antibody against RAGE, goat polyclonal antibodies against actin (C-11) and HRP-labeled secondary antibodies were purchased from Santa Cruz Biotechnology Inc. (Santa Cruz, CA). Total protein measurement's reagents with the bicinchoninic acid (BCA) method were from Pierce (Rockford, IL). All other chemicals and reagents were of analytical grade and were readily available from commercial sources.

Animals. Sprague Dawley male rats from Harlan Laboratories (Houston, TX) were used for the experiments of isolation of hepatocytes from entire liver. Rats age were around 2-3 months with average weight between 260 to 340 g. Animals were allowed to easy access for

water and standard food and maintained at 22^{o}C, 35% relative humidity and 12 h dark/light cycle. All animal experiments were approved by the Institutional Animal Care and Use Committee of the University of Louisiana at Monroe and all surgical procedures were consistent with the IACUC policies and procedures.

Isolation of Primary Rat Hepatocytes. The isolation and purification procedures of hepatocytes from animals' livers were done under aseptic condition. The animal was anesthetized with IP injection of 0.06 g/kg ketamine/0.012 g/kg xylazine, then the liver portal vein was canulated and perfusion was started following the two-step collagenase perfusion technique previously described (Seglen, 1976). First, the liver was perfused with a 450 ml of Ca^{++}-free Hanks Balanced Salt Solution (HBSS) buffer containing 1 mM ethylene glycol tetraacetic acid (EGTA) and 0.022 mg/ml heparin neutralized to pH 7.4 at flow rate of 35 ml/min. Immediately after that the liver was perfused with 350 ml standard HBSS supplemented with 5 mM $CaCl_2$, 100 U/ml collagenase type-I, and 70 mg soybean trypsin inhibitor at flow rate of 30 ml/min. All solutions and tubing were maintained at 37^{o}C and saturated with 95%O_2/5%CO_2. Following the perfusion step, the liver was excised and put in a dish containing warm DMEM supplemented with 5%FBS, 100 U/ml penicillin, 100 g/ml streptomycin, 4 mg/l insulin, and 1 µM dexamethasone, and placed on ice to reach 4^{o}C. The liver capsule was stripped slowly and cells were released by gently combing the liver with a steel comb. Cells were filtered through 70 µm mesh and hepatocytes were separated from other liver cells population by centrifugation at 50 x *g* for 5 min twice, followed by centrifugation with 35% percol solution to remove dead cells. Hepatocytes were resuspended in serum-free medium and viability was determined using trypan blue method.

DMD Fast Forward. Published on July 12, 2013 as DOI: 10.1124/dmd.113.052514
This article has not been copyedited and formatted. The final version may differ from this version.

Preparation of Sandwich Cultured Primary Rat Hepatocytes. All culture plates were pre-coated with thin collagen layer as a matrix for hepatocytes attachment. Twenty four and 6-well plates were coated with 300 and 1400 µl of 50 µg/ml collagen in 0.2 M acetic acid solution, respectively, and left to dry overnight inside the hood. Plates were then neutralized and washed twice with sterile distilled water, and then 0.5 ml/well of DMEM were added and plates were incubated at 37^{o}C for 2 to 3 h to hydrate the collagen layer before seeding the cells. Hepatocytes were seeded at 0.7x10^{6} cells/ml and allowed to attach for 1 to 2 h. The medium was then aspirated to remove unattached dead cells followed by addition of 0.5 ml/well of fresh medium (DMEM supplemented with 5% FBS, 100 U/ml penicillin, 100 g/ml streptomycin, 4 mg/l insulin, and 1µM dexamethasone) and incubated for 6 h. Medium was then replaced with serum-free medium supplemented with 1% ITS, 100 U/ml penicillin, 100 g/ml streptomycin, and 0.1 µM dexamethasone. Twenty four hours later, the medium was removed and hepatocytes were overlaid with 0.5 ml of 0.25 mg/ml matrigel in ice-cold medium and incubated at 37^{o}C for 24 h, after which medium was replaced with fresh medium everyday up to day 4 where activity studies or protein extraction for western blot were performed.

Validation of Sandwich Cultured Primary Rat Hepatocytes Model.

Light microscopy imaging: To confirm the integrity of canalicular networks, phase-contrast microscopy images were taken in day 4 of SCHs using Nikon Eclipse TS100 inverted microscope from EquipNet, Inc. (Canton, MA).

Fluorescence microscopy imaging: 5-(and-6)-carboxy-2',7'-dichlorofluorescein diacetate (CDFDA) was used as a canalicular marker in SCHs on day 4. CDFDA is passively uptaken into hepatocytes and metabolized into the fluorescent metabolite 5-(and-6)-carboxy-2',7'-dichlorofluorescein (CDF), which is actively effluxed into the canalicular space via multidrug

DMD Fast Forward. Published on July 12, 2013 as DOI: 10.1124/dmd.113.052514
This article has not been copyedited and formatted. The final version may differ from this version.

resistance-associated protein 2, MRP2 (Liu et al., 1999b). In these experiments, a culture plate was rinsed with standard HBSS and incubated in the same buffer for 10 min. After aspiration of the buffer, 2 μM CDFDA dissolved in HBSS containing 5mM $CaCl_2$ was added to the cells and incubated for 10 min followed by aspiration and 4 times washing with ice-cold standard HBSS. Images were then captured for accumulated CDF into canalicular spaces using inverted microscope Olympus 1x71 (Center Valley, PA) at 20X magnification.

Cumulative uptake of [^{3}H] taurocholate and [^{14}C] salicylic acid in SCHs as positive and negative controls, respectively: On day 4 of SCHs, cells were washed with warm standard HBSS (i.e. contains 5 mM $CaCl_2$) or Ca^{++}-free HBSS containing EDTA, and then incubated in their respective buffers for 5 min. Subsequently, 1 μM of either [^{3}H] taurocholate or [^{14}C] salicylic acid were dissolved in HBSS with or without calcium and added to the cells. After 10 min incubation at 37^{o}C plates were placed on ice and uptake was ended by aspirating the incubation medium and washing wells four times with ice-cold standard HBSS. Cells were lysed by adding 200 μl RIPA buffer (25 mM Tris HCl, 150 mM NaCl, 1% NP-40, 1% sodium deoxylate, 0.1% SDS, pH 7.6) containing 1% protease inhibitors cocktail, sonicated for 30 s, and incubated on ice with shaking for 2 h. Samples were analyzed using Wallac 1414 WinSpectral Liquid Scintillation Counter (PerkinElmer Inc.; Waltham, MA). Data were normalized to protein content in each well using BCA protein assay kit with bovine serum albumin (BSA) as standard.

Canalicular efflux of rhodamine123 (Rh123): Rh123 is passively uptaken into hepatocytes and its biliary excretion is mediated by P-gp (Annaert and Brouwer, 2005). On day 4, SCHs in 6-well plate were rinsed twice in standard HBSS and incubated in the same buffer for 10 min. Subsequently, the buffer was aspirated and cells were preloaded with 1 μM Rh123 dissolved into standard HBSS for 30 min followed by aspiration of the incubation medium and

washing four times with ice-cold HBSS. Afterward, efflux study was initiated by incubating the cells in warm HBSS with or without calcium for 30 min at 37^{o}C. At the end of the incubation time, aliquots from incubation medium were measured for fluorescent intensity of Rh123 using Synergy 2 microplate reader (Biotek, Winooski, VT) with excitation and emission wavelengths of 485 and 529 nm, respectively. Data acquisition was achieved using Gene5 software (Biotek). Data were normalized to protein content in each well and the BEI% of Rh123 was calculated using equation 1 described below under data analysis.

Western Blot Analysis. Hepatocytes were seeded in 6-well plates and maintained up to 4 days in sandwich configuration. In case of induction studies with rifampicin, hepatocytes were cultured in sandwich configuration for 2 days, and then rifampicin treatment (50 μM) was initiated and added freshly everyday up to day 4 of sandwich culture. Subsequently, media were removed and cells were washed twice using ice-cold HBSS, scraped, collected in 1.5 ml eppendorf tube, and then centrifuged at 2000 x *g* for 10 min at 4°C. The cells pellets were then re-suspended and homogenized in RIPA buffer containing 1% protease inhibitors cocktail and incubated on ice for 1 h. The samples were then centrifuged at 15,000 x *g* for 15 min at 4°C. The lysate samples were stored at -80°C for subsequent Western blot analyses. Twenty five micrograms of protein samples were loaded and resolved using 7.5% SDS-polyacrylamide gel with a 5% stacking gel at 140 V for 1 h. Proteins were transferred electrophoretically onto nitrocellulose membranes at 300 mA for 1.5 h. After that, the membranes were blocked by incubation with 2% BSA on rocking platform for 1 h at room temperature followed by incubation with the primary antibodies RAGE IgG (N-16), P-gp (C-219), LRP1 (light chain), or β-actin (C-11) at dilutions 1: 125, 1: 200, 1: 1500, and 1: 3000, respectively, in PBS containing 2% BSA and 0.05% Tween-20 overnight at 4°C. For proteins detection, membranes were

DMD Fast Forward. Published on July 12, 2013 as DOI: 10.1124/dmd.113.052514
This article has not been copyedited and formatted. The final version may differ from this version.

incubated with secondary anti-mouse IgG antibody for P-gp, and anti-goat IgG antibody for RAGE and β-actin, or with anti-rabbit IgG antibody for LRP1, all labeled with horseradish peroxidase (HRP), at 1:5000 dilution for P-gp, RAGE and β-actin or 1: 2000 dilution for LRP1 for 1 h at room temperature. The blots were developed using a chemiluminescence detection kit (SuperSignal West Femto substrate; Thermo Scientific, Waltham, MA). Quantitative analysis of the immunoreactive bands was performed using Syngene luminescent image analyzer (Scientific Resources Southwest, Inc.; Stafford, TX). Protein quantification was performed and data were expressed as ratio of proteins to β-actin.

Immunocytochemistry of RAGE. SCHs cultured for 4 days were fixed in a 2% glutaraldehyde in PBS solution for 30 min at room temperature, followed by incubation with a 0.1% Triton X100 solution for membrane permeabilization. The SCHs samples were placed in a blocking solution of 1% BSA in PBS solution for 1 h at 37^{o}C. The cells were first exposed to RAGE (A-9) primary mouse monoclonal antibody (Santa Cruz Biotechnology) for 2 h at 37^{o}C and subsequently exposed to a FITC-conjugated goat anti-mouse secondary antibody (Santa Cruz Biotechnology) for 1 h at room temperature. Images were acquired by Nikon Eclipse fluorescent microscope.

Time Dependent Studies of ^{125}I-Aβ40 Accumulation in Conventional and Sandwich Cultured Primary Rat Hepatocytes. Time dependent accumulation studies of ^{125}I-Aβ_{40} in SCHs were performed on day 4. Cells were incubated with 0.5 ml of 0.14 nM ^{125}I-Aβ_{40} prepared in standard or Ca^{++}-free HBSS. Following 5, 15, 30 and 60 min incubation times, cells were lysed and counted for radioactivity. To study the effect of calcium on the cumulative uptake of ^{125}I-Aβ_{40}, conventional cultured hepatocytes were prepared in a 24-well plate. In this case hepatocytes were not overlaid with a second matrix layer, but rather they were seeded on hard

DMD Fast Forward. Published on July 12, 2013 as DOI: 10.1124/dmd.113.052514
This article has not been copyedited and formatted. The final version may differ from this version.

collagen coated plates to spread as monolayers. At the same time hepatocytes were seeded on another plate and overlaid with matrigel layer to obtain sandwich configuration. The two plates were incubated for 2 days when 0.5 ml of 0.14 nM ^{125}I-Aβ_{40} were added to the cells, with or without calcium, and incubated for 5 and 30 min at 37^{o}C. Uptake were ended by aspirating the medium and washing the cells with ice cold standard HBSS while keeping plates on ice. Cells were lysed and quantitative determination of intracellular ^{125}I-Aβ_{40} accumulations were performed as mentioned above. Degradation of ^{125}I-Aβ_{40} was determined by trichloroacetic acid (TCA) precipitation assay (Shibata et al., 2000). Cells lysate samples were mixed (1:1 volume) with TCA (final concentration 10%) and centrifuged at 14,000 x *g* at 4°C for 10 min. Radioactivity in the supernatant was determined using Wallac 1470 Wizard Gamma Counter (PerkinElmer Inc.).

Determination of the Biliary Excretion Index (BEI) and Biliary Clearance (Cl_{bile}) of ^{125}I-Aβ_{40}. All experiments have their own control and were conducted on day 4 of sandwich culture. Twenty four well plates were preincubated in standard or Ca^{++}-free HBSS for 5 min. Subsequently, 0.5 ml of 0.14 nM ^{125}I-Aβ_{40} in standard or Ca^{++}-free HBSS were added to cell culture plates and incubated for 30 min at 37^{o}C. Uptake was stopped by placing plates on ice and removal of incubation medium and washing cells three times with ice-cold standard HBSS containing 0.2%BSA and once with standard HBSS only to remove BSA residue. Cells were then lysed by addition of RIPA buffer containing 1% protease inhibitors cocktail, sonicated for 30 s followed by gentle shaking on rocking platform for 2 h at 4^{o}C. Intracellular radioactivity of ^{125}I-Aβ_{40} was measured using Wallac 1470 Wizard Gamma Counter. Data obtained were normalized to protein content. Results were also normalized to ^{125}I-Aβ_{40} non-specific matrigel binding by subtracting ^{125}I-Aβ_{40} bound to matrigel coated wells without cells. Non-specific

DMD Fast Forward. Published on July 12, 2013 as DOI: 10.1124/dmd.113.052514
This article has not been copyedited and formatted. The final version may differ from this version.

binding was found to be less that 2%. The obtained data from the accumulation experiments of ^{125}I-Aβ_{40}, in the presence or absence of calcium, were used to calculate BEI using equation 2 and biliary clearance (Cl_{bile}) using equation 3 described below under data analysis.

Effect of Transport Proteins Inhibition on ^{125}I-Aβ_{40} BEI and Cl_{bile} in SCHs. For P-gp inhibition studies, verapamil (50 μM) or valspodar (20 μM) were used, while for LRP1 and RAGE inhibition, RAP (1 μM) and RAGE IgG antibody (10 μg/ml) were used, respectively. In these experiments, cells were washed with warm standard or Ca^{++}-free HBSS, and incubated in their respective buffers for 5 min at 37^{o}C. Then buffers were removed and replaced with 0.5 ml of 0.14 nM ^{125}I-Aβ_{40} alone or with inhibitors, and incubated for 30 min at 37^{o}C. Subsequently, plates were placed on ice and medium was removed by aspiration and cells were washed three times with ice-cold 0.2% BSA in standard HBSS and once with standard HBSS to remove BSA residues. Cells were then lysed and used for ^{125}I-Aβ_{40} quantification by gamma counter.

Effect of P-gp Induction by Rifampicin on ^{125}I-Aβ_{40} BEI and Cl_{bile} in SCHs. Twenty four well plates of SCHs were treated with or without 50 μM rifampicin dissolved into serum-free DMEM (supplemented with 1%ITS, 100U/ml penicillin, 100 g/ml streptomycin, and 1μM dexamethasone) for 48 h, starting from day 2 of sandwich culture. After the end of treatment on day 4 of culture, medium was removed and replaced with freshly prepared medium and incubated for 8 h as washout period. Consequently, Medium was removed by aspiration and cells were rinsed gently with warm standard or Ca^{++}-free HBSS, and incubated in their respective buffers for 5 min at 37^{o}C/5% CO_2. Cumulative uptake was initiated by adding 0.5 ml/well of 0.14 nM ^{125}I-Aβ_{40} with or without calcium for 30 min at 37^{o}C. Similarly, for inhibition study, verapamil (50 μM) was co-incubated with 0.14 nM ^{125}I-Aβ_{40} for 30 min. At the end of

DMD Fast Forward. Published on July 12, 2013 as DOI: 10.1124/dmd.113.052514
This article has not been copyedited and formatted. The final version may differ from this version.

experiment, ^{125}I-Aβ_{40} radioactivity was determined in the cell lysate and BEI% and Cl_{bile} were calculated according to equations 2 and 3, respectively.

Data Analysis. Efflux of substrates into canalicular spaces in SCHs (i.e. BEI %) was determined by the cumulative efflux or cumulative uptake method. For Rh123, BEI was determined using the cumulative efflux method (Liu et al., 1999b) where the cumulative efflux of Rh123 into Ca^{++}-free HBSS (cells+canaliculi) and standard HBSS (cells only) were determined. Their difference represents the canalicular efflux as shown in equation 1.

$$\textbf{BEI\%} = \frac{\textbf{Efflux from cells+canaliculi } (\textbf{-Ca}^{++}) \textbf{- Efflux from cells } (\textbf{+Ca}^{++})}{\textbf{Efflux from cells+canaliculi } (\textbf{-Ca}^{++})} \textbf{ x 100} \qquad \textbf{(1)}$$

For ^{125}I-Aβ_{40}, [^{3}H] taurocholate, and [^{14}C] salicylic acid the canalicular efflux was determined by the cumulative uptake method (Liu et al., 1999b). In this case, uptake of a substrate prepared in calcium containing buffer by SCHs represents its accumulation into cells and canalicular lumen, while the uptake of this substrate prepared in calcium- free buffer represents its accumulation into cells only. The difference in readings between both treatments was used to calculate the BEI% and Cl_{bile} as shown in equations 2 and 3, respectively. In equation 3, AUC_{medium} was determined as the product of the incubation time and substrate initial concentration in the incubation medium.

$$\textbf{BEI\%} = \frac{\textbf{Accumulation into cells+canaliculi } (\textbf{+Ca}^{++}) \textbf{- Accumulation into cells } (\textbf{-Ca}^{++})}{\textbf{Accumulation into cells+Canaliculi } (\textbf{+Ca}^{++})} \textbf{ x 100} \qquad \textbf{(2)}$$

$$\textbf{Cl}_{\textbf{bile}} = \frac{\textbf{Accumulation into cells+canaliculi } (\textbf{+Ca}^{++}) \textbf{- Accumulation into cells } (\textbf{-Ca}^{++})}{\textbf{AUC}_{\textbf{medium}}} \qquad \textbf{(3)}$$

All biliary clearance values are reported with the unit ml/min/kg body weight based on 200 mg of protein/g of liver and 40 g of liver/kg of rat body weight (Seglen, 1976).

Statistical Analysis. Unless otherwise indicated, all data were expressed as mean ± SEM. The experimental results were statistically analyzed for significant difference using unpaired two-tailed Student's t-test for two groups, and one-way analysis of variance (ANOVA) followed by the Bonferroni's test for more than two groups analysis. A P-value less than 0.05 were considered statistically significant.

DMD Fast Forward. Published on July 12, 2013 as DOI: 10.1124/dmd.113.052514
This article has not been copyedited and formatted. The final version may differ from this version.

Results

SCHs Model Validation. Formation of canalicular networks was confirmed by light microscopy imaging. Fig. 1A shows canalicular space formation as bright white spaces indicated by the small white arrow. The content of the canalicular space is sealed by the tight junctions as shown in Fig. 1B, where the canalicular marker CDFDA was passively uptaken inside the hepatocytes and rapidly metabolized to the fluorescent CDF which is effluxed into the canalicular space via MRP2, expressed on the apical side of hepatocytes confirming the canalicular spaces formation (Liu et al., 1999b). Levels of P-gp, LRP1 and RAGE protein expression in SCHs cultured for 4 days were determined by Western blot analysis. P-gp, LRP1, RAGE, and β-actin protein were detected at 150, 85, 55 and 46 kDa, respectively, as shown in Fig. 2.

The activity of the sandwich culture was further tested by using the bile salt [^{3}H] taurocholate for active transport, and [^{14}C] salicylic acid as a passive diffusion marker that is not excreted in the bile canaliculi. Consistent with other studies in the literature (Liu et al., 1999a), the BEI% of [^{3}H] taurocholate was as high as 52.7±8.2% whereas for [^{14}C] salicylic acid was approximately zero as its cellular accumulation with or without calcium was approximately the same (Fig. 3A). The Cl_{bile} of [^{3}H] taurocholate was also determined in SCHs on day 4 of culture and was 81.0±7.7 ml/min/kg.

The functional activity of P-gp at the apical side of the SCHs was determined by using the specific substrate Rh123. Efflux of 1 μM Rh123 into the incubation buffer in presence or absence of calcium was performed and the BEI% was calculated to be 19.4±5.2% with a significant difference in its efflux between both incubation buffers ($P<0.05$) (Fig. 3B).

DMD Fast Forward. Published on July 12, 2013 as DOI: 10.1124/dmd.113.052514
This article has not been copyedited and formatted. The final version may differ from this version.

Determination of ^{125}I-Aβ_{40} Biliary Excretion (BEI), biliary clearance ($Cl_{bile)}$, and Cumulative Uptake. To determine Aβ hepatic transport mechanisms, ^{125}I-labeled Aβ_{40} was used for sensitive quantification. Bell et al have shown that ^{125}I-labeling of Aβ_{40} did not alter the transport properties of ^{125}I-Aβ_{40} compared to the unlabeled peptide, and that the clearance rates of both peptides were identical (Bell et al., 2007). In addition, free Aβ_{40} instead of Aβ_{40}-sLRP1 complex was investigated in the current studies to imitate mild cognitive impairment (MCI) and AD condition where, unlike in normal physiologic condition, sLRP1 is mostly present in oxidized form with negligible binding affinity to Aβ_{40} causing sharp increase in free Aβ_{40} plasma levels (Sagare et al., 2011). Although Aβ_{42} is more prone to aggregation compared to Aβ_{40}, both Aβ peptides have been implicated in the pathogenesis of AD (Hardy, 2006), and participate in the formation of senile plaques with neurotoxicity potentials (Chiang et al., 2008; Seeman and Seeman, 2011). Aβ_{40} and Aβ_{42} are substrates for P-gp and LRP1 (Cirrito et al., 2005; Shibata et al., 2000), thus both peptides clearance is expected to be altered by these transport proteins modulations. In this study, Aβ_{40} was used in the BEI experiments for practicality reasons as it has much faster clearance rate than Aβ_{42} (Ito et al., 2006; Zlokovic et al., 2000).

To determine the optimum time (when steady state achieved) for ^{125}I-Aβ_{40} biliary excretion measurement, time course accumulation with or without calcium were performed and biliary excretion was determined at different time points. As shown in Fig. 4, the biliary excretion of ^{125}I-Aβ_{40} was time dependent and reached steady state at 30 min with a BEI% and Cl_{bile} values of 29.8±2.3 % and 1.47ml/min/kg, respectively. Thus, all subsequent cumulative uptake and BEI% studies were conducted at 30 min incubation time. To evaluate the effect of calcium on the cumulative uptake of ^{125}I-Aβ_{40}, conventional hepatocyte culture (i.e. not in sandwich configuration) was seeded in parallel with SCHs and maintained for 48 h at 37^{o}C.

DMD Fast Forward. Published on July 12, 2013 as DOI: 10.1124/dmd.113.052514
This article has not been copyedited and formatted. The final version may differ from this version.

Forty eight hours culture time was selected as the viability and functionality of conventionally cultured primary hepatocytes start to decline at longer time (Hewitt et al., 2007; Swift et al., 2010). As shown in Fig. 5A, the difference between ^{125}I-Aβ_{40} cumulative uptake in the presence or absence of calcium in the conventional model was insignificant at 5 and 30 min suggesting no effect of calcium on ^{125}I-Aβ_{40} uptake; however the cumulative uptake in SCHs while not different at 5 min, the difference was obvious and significant at 30 min incubation time demonstrating excretion of ^{125}I-Aβ_{40} into canalicular spaces that were maintained only in the presence of calcium. Using the TCA assay, percent of ^{125}I-Aβ_{40} intracellular degradation was determined and ranged from 27 to 36% (Fig. 5A, $P>0.05$). It was observed that ^{125}I-Aβ_{40} intracellular degradation after 30 min of cumulative uptake decreased significantly ($\simeq$17%) in SCHs at day 4 compared to 27% degradation at day 2 of sandwich culture ($P<0.05$). On the other hand, the BEI% of total ^{125}I-Aβ_{40} (intact+ degraded) increased significantly with time of culture, with 19.4±3.6% and 27.5±2.9% ($P<0.05$) for SCHs at day 2 and 4, respectively (Fig. 5B).

Effect of Transport Proteins Inhibition on ^{125}I-Aβ_{40} BEI and Cl_{bile} in SCHs. Inhibition studies of major ^{125}I-Aβ_{40} transport proteins were conducted to investigate the effect of such inhibition on ^{125}I-Aβ_{40} cellular accumulation and biliary excretion. Fig. 6 illustrates the effect of P-gp inhibition by verapamil or valspodar on ^{125}I-Aβ_{40} biliary excretion in SCHs. Verapamil (50 μM) caused a significant reduction in ^{125}I-Aβ_{40} BEI% from 27.1±4.1% to 12.4±1.4% ($P<0.05$). The role of P-gp mediated canalicular efflux of ^{125}I-Aβ_{40} was further confirmed with the selective inhibitor valspodar. Similarly, valspodar (20 μM) significantly reduced ^{125}I-Aβ_{40} BEI% from 27.1±4.1% to 9.6±2.6% ($P<0.01$).

Furthermore, the role of LRP1 and RAGE in mediating the ^{125}I-Aβ_{40} disposition in SCHs was assessed using specific inhibitors. As shown in Fig. 7, RAGE antibody (10 μg/ml)

DMD Fast Forward. Published on July 12, 2013 as DOI: 10.1124/dmd.113.052514
This article has not been copyedited and formatted. The final version may differ from this version.

reduced the BEI% and Cl_{bile} of ^{125}I-$A\beta_{40}$ from 27.1±4.6% to 20.6±2.6% and from 1.5±0.06 to 0.9±0.09 ml/min/kg, respectively. Co-incubation of ^{125}I-$A\beta_{40}$ with 2 μM RAP, a known chaperone molecule for LRP1 and a competitive inhibitor for Aβ as determined previously (Qosa et al., 2012; Shibata et al., 2000), caused a significant reduction in the BEI% and Cl_{bile} of ^{125}I-$A\beta_{40}$ by approximately 2.4-fold (from 27.1±4.6% to 11.2±4.8%) and 2.7-fold (from 1.5±0.06 to 0.5±0.15 ml/min/kg) ($P<0.01$), respectively. Both inhibitors, RAP and RAGE-IgG, showed a comparable inhibition of $A\beta_{40}$ cumulative uptake in the presence of calcium compared to control (Fig. 7, black bars), while its cumulative uptake in the absence of calcium between the three groups (Fig. 7, grey bars) was not significantly different indicating that the effect of both inhibitors was on $A\beta_{40}$ uptake from the sinusoidal side of hepatocytes. However, based on the difference in $A\beta_{40}$ cumulative uptakes in the presence and absence of calcium, the Cl_{bile} of $A\beta_{40}$ with LRP1 inhibitor was significantly lower than its Cl_{bile} with RAGE inhibitor ($P<0.01$) suggesting the greater role of LRP1 in $A\beta_{40}$ cellular uptake compared to RAGE.

TCA studies, on the other hand, revealed that P-gp, LRP1, and RAGE inhibition did not alter the degradation % of $A\beta_{40}$ (~17%) demonstrating that $A\beta_{40}$ degradation products are not substrates for these transport proteins.

RAGE localization in the SCHs was investigated and confirmed by immunocytochemistry. The results demonstrated RAGE distribution at the sinusoidal side of the SCHs (green fluorescence, Fig. 8), and was not detected at the bile canaliculi (white arrows, Fig. 8).

Effect of Rifampicin Treatment on ^{125}I-$A\beta_{40}$ BEI% and Cl_{bile} in SCHs. Rifampicin (50 μM) treatment significantly increased the expression of P-gp and LRP1 by 1.6- and 1.4-fold,

DMD Fast Forward. Published on July 12, 2013 as DOI: 10.1124/dmd.113.052514
This article has not been copyedited and formatted. The final version may differ from this version.

respectively, but not RAGE expression (Fig. 2). This increase in expression was associated with enhanced BEI% and Cl_{bile} of ^{125}I-Aβ_{40} when compared to vehicle treated cells. The BEI% and Cl_{bile} of ^{125}I-Aβ_{40} were significantly increased from 30.2±2.2% to 38.2±1.3%, and from 1.5±0.15 to 1.8±0.2 ml/min/kg, respectively, ($P<0.05$). P-gp inhibition by verapamil caused a significant decrease in the BEI in both control and rifampicin treated cells, with more pronounced inhibitory effect on rifampicin treated cells. As shown in Fig. 9, the BEI% of ^{125}I-Aβ_{40} was significantly reduced from 30.2±2.2% to 17.4±0.7% ($P<0.01$), and from 38.2±1.3% to 7.8±1.1% ($P<0.001$) in control and rifampicin treated cells, respectively.

DMD Fast Forward. Published on July 12, 2013 as DOI: 10.1124/dmd.113.052514
This article has not been copyedited and formatted. The final version may differ from this version.

Discussion

Understanding Aβ hepatic transport mechanisms might unravel novel therapeutic targets to enhance Aβ systemic elimination through the liver and consequently reduce its burden in the brain (Sehgal et al., 2012). While available studies mostly focused on the role of LRP1 in hepatocellular uptake of $A\beta_{40}$, the contribution of P-gp and RAGE, transport proteins that have established functions in Aβ transport across BBB, to the hepatic clearance of Aβ is poorly understood. Thus, to further characterize the role of these transport proteins and their interplay in $A\beta_{40}$ hepatic clearance, primary rat hepatocytes cultured in sandwich configuration were utilized.

SCHs was optimized and validated for formation of canalicular networks by observing the formation of canalicular spaces under light microscopy as well as by accumulation of the fluorescent metabolite CDF (Fig. 1). Also, BEI% and Cl_{bile} measurements of [^{3}H] taurocholate and [^{14}C] salicylic acid, used as positive and negative controls, respectively, were in agreement with previous work (Liu et al., 1999a; Turncliff et al., 2006); and the functional activity of P-gp, determined using Rh123 as a model substrate, was consistent with previously reported results (Annaert and Brouwer, 2005).

This *in vitro* model was successfully used to determine the BEI% of ^{125}I-$A\beta_{40}$ for the first time. Treating SCHs with ^{125}I-$A\beta_{40}$ for 30 min demonstrated significantly higher accumulation of ^{125}I-$A\beta_{40}$ in HBSS containing calcium compared to calcium-free HBSS with a BEI% of 29.8±2.3%, which is considered moderate as compared to [^{3}H] taurocholate (52.7±8.2%) and Rh123 (19.4±5.2%) (Fig. 3). The effect of calcium on the difference in ^{125}I-$A\beta_{40}$ uptake in SCHs was rolled out by performing cumulative uptake studies of ^{125}I-$A\beta_{40}$ with or without calcium in primary hepatocytes cultured in conventional culture and was compared to SCHs. Degradation

DMD Fast Forward. Published on July 12, 2013 as DOI: 10.1124/dmd.113.052514
This article has not been copyedited and formatted. The final version may differ from this version.

studies by TCA assay suggested biliary excreted ^{125}I-Aβ_{40} was mostly intact (~85%) supported by the intracellular degradation and modulation studies; however the degradation of ^{125}I-Aβ_{40} in SCHs decreased with culture time. While further studies are required to explain this observation, this decrease could be due to reduced expression of Aβ_{40} degrading enzymes such as NEP and IDE with culture time, an observation that has been reported previously in SCHs with other enzymes including CYP450 (Hewitt et al., 2007), or reduced expression of another uptake mechanism coupled with Aβ_{40} endocytotic degradation.

Consistent with available studies in rats (Tamaki et al., 2006; Tamaki et al., 2007) and transgenic mice (Sehgal et al., 2012), our data demonstrated basolateral LRP1 to play an important role in mediating the hepatic clearance of Aβ_{40} from the general circulation and was confirmed by inhibition studies. RAP significantly reduced ^{125}I-Aβ_{40} BEI% and Cl_{bile} by 2.4- and 2.7-fold, respectively. Interestingly, the same concentration of RAP (2 μM) was reported to decrease the liver uptake of intravenously administered ^{125}I-Aβ_{40} by 48% (~2-fold) in rats (Tamaki et al., 2006), which is in agreement with our finding. Another interesting finding is that LRP1 inhibition did not affect ^{125}I-Aβ_{40} degradation in SCHs (~15% in absence and presence of RAP) suggesting that LRP1 mediates transcytosis of intact ^{125}I-Aβ_{40} in SCHs. Similar observation was reported previously by Pflanzner and colleagues who used primary mouse brain capillary endothelial cells grown on filters and showed that LRP1-mediates intact Aβ_{40} transport by transcytosis and play no role in its degradation in this model (Pflanzner et al., 2011).

P-gp is expressed abundantly on the canalicular side of hepatocytes, and Aβ_{40} is a P-gp substrate (Lam et al., 2001). P-gp at the apical side of BBB has been shown to play a substantial role in controlling Aβ levels in the brain by enhancing its removal from brain to blood, and by limiting Aβ access to the brain (Abuznait et al., 2011; Cirrito et al., 2005; Kuhnke et al., 2007).

DMD Fast Forward. Published on July 12, 2013 as DOI: 10.1124/dmd.113.052514
This article has not been copyedited and formatted. The final version may differ from this version.

To study the role of P-gp in the canalicular excretion of $A\beta_{40}$, two potent P-gp inhibitors, verapamil and valspodar, were used. Verapamil inhibition of P-gp has been reported in various *in vitro* models including SCHs (Annaert and Brouwer, 2005), Caco2 cells (Bansal et al., 2009), and LLC-PK1 cells expressing human *MDR1* (Sugimoto et al., 2011). Also, valspodar was demonstrated as an effective P-gp inhibitor in MDCKII-MDR1 and rat brain microcapillary endothelial cells (Sziraki et al., 2011). Both compounds inhibited P-gp efflux function and significantly reduced the BEI% of ^{125}I-$A\beta_{40}$ with more pronounced effect demonstrated by valspodar compared to verapamil with 64 and 54% reductions, respectively. The reduction in BEI% with both inhibitors can also be noticed from the significant increase in the accumulation of ^{125}I-$A\beta_{40}$ in calcium-free HBSS, from 2.0±0.04 to 2.5±0.2 ($P<0.01$) and 2.2±0.04 ($P<0.05$) fmol/mg protein for valspodar and verapamil treated cells, respectively (Fig. 6). In the absence of calcium, the tight junctions are disrupted and the canalicular ^{125}I-$A\beta_{40}$ is released into the medium during incubation which is consequently removed by washing at end of experiment and hence, any increase in ^{125}I-$A\beta_{40}$ accumulation inside the cells in the absence of calcium is due to the specific inhibition of canalicular efflux of ^{125}I-$A\beta_{40}$ through apical P-gp. To our knowledge, this function of canalicular P-gp in the hepatic clearance of $A\beta_{40}$ is first to be shown by this study.

We also tested the role of RAGE in mediating ^{125}I-$A\beta_{40}$ clearance in SCHs. According to our knowledge, RAGE localization in hepatocytes has not been identified. In this study, we have successfully confirmed its sinusoidal localization in SCHs at day 4 by immunocytochemistry (Fig. 8). Inhibition studies with RAGE antibody showed a reduction by 24% and 36% in ^{125}I-$A\beta_{40}$ BEI% and Cl_{bile}, respectively ($p<0.05$), demonstrating significantly less role in mediating the hepatic clearance of ^{125}I-$A\beta_{40}$ than that of LRP1.

DMD Fast Forward. Published on July 12, 2013 as DOI: 10.1124/dmd.113.052514
This article has not been copyedited and formatted. The final version may differ from this version.

Collectively, the above observations confirm hepatic LRP1 and P-gp as significant players in determining Aβ systemic levels, and suggest that a small decline in their expression and/or activity could decrease Aβ systemic clearance and possible contribution to Aβ accumulation in the brain. Considering the established role of age-associated decline in LRP1 and P-gp mediated removal of Aβ peptides in human (Vogelgesang et al., 2002) and rats (Silverberg et al., 2010), strategies to up-regulate both proteins expression and/or activity at the BBB have been investigated as a potential preventive approach (Hartz et al., 2010; Qosa et al., 2012). *In vivo* brain efflux index studies conducted on C57BL/6 mice treated with rifampicin or caffeine significantly enhanced $A\beta_{40}$ clearance by more than 20% when compared to control vehicle treated mice (Qosa et al., 2012). Thus, in the current study we investigated the effect of both proteins up-regulation by rifampicin on the hepatic clearance of $A\beta_{40}$. Rifampicin treatment increased the expression of LRP1and P-gp but not RAGE, and was reflected on ^{125}I-$A\beta_{40}$ disposition in SCHs. Biliary clearance and excretion of ^{125}I-$A\beta_{40}$ were significantly increased by rifampicin due to enhanced functional activity of LRP1 at the basolateral side and P-gp at the apical side of hepatocytes. These results are consistent with our previous study where mice treatment with rifampicin for 3 weeks increased LRP1and P-gp expression at the BBB and was associated with enhanced clearance of ^{125}I-$A\beta_{40}$ across the BBB (Qosa et al., 2012). Interestingly and consistent with our *in vivo* study findings (Qosa et al., 2012), P-gp inhibition with verapamil significantly reduced ^{125}I-$A\beta_{40}$ BEI% by 80% in rifampicin treated cells compared to 43% in vehicle treated cells indicating that rifampicin induced another mechanism that plays important role in ^{125}I-$A\beta_{40}$ clearance and was inhibited by verapamil. Further studies are in progress to explain this observation. Accordingly, similar to BBB role in maintaining Aβ homeostasis in the brain, the role of hepatic clearance is very important in maintaining Aβ homeostasis in the body.

DMD Fast Forward. Published on July 12, 2013 as DOI: 10.1124/dmd.113.052514
This article has not been copyedited and formatted. The final version may differ from this version.

As the level of LRP1 and P-gp expressions decrease with aging and in AD (Silverberg et al., 2010; Toornvliet et al., 2006), the level of Aβ is expected to increase in the general circulation as a result of insufficient systemic clearance (Mackic et al., 1998; Tamaki et al., 2006), which may allow for more Aβ influx into the brain. Our results demonstrated that modulation of LRP1 and/or P-gp alters $A\beta_{40}$ biliary clearance and excretion supporting their important function in regulating $A\beta_{40}$ systemic levels, and that their up-regulation present a novel therapeutic approach for AD prevention and treatment. Furthermore, our findings suggest that while the hepatic disposition of $A\beta_{40}$ is mediated by several transport proteins, competition with endogenous and exogenous substances that are mainly eliminated via similar transport system in the liver might hinder Aβ hepatic clearance and contribute to the elevated levels of systemic Aβ observed in Alzheimer's patients.

In summary, our data showed that beside LRP1, P-gp is involved in the biliary excretion of $A\beta_{40}$ in SCHs. Furthermore, the present study demonstrated that $A\beta_{40}$ uptake in SCHs is mediated mainly by LRP1 and to a much lesser extent by RAGE. P-gp is not only involved in the clearance of $A\beta_{40}$ across the BBB but also in its biliary excretion, and its role was confirmed by inhibition and induction studies. Furthermore, SCHs provided a useful *in vitro* model to differentiate between $A\beta_{40}$ sinusoidal and canalicular disposition and successfully determined its biliary excretion.

Authorship Contributions

Participated in research design: Mohamed and Kaddoumi

Conducted experiments: Mohamed

Performed data analysis: Mohamed

Wrote or contributed to the writing of the manuscript: Mohamed and Kaddoumi

References

Abuznait AH, Cain C, Ingram D, Burk D and Kaddoumi A (2011) Up-regulation of P-glycoprotein reduces intracellular accumulation of beta amyloid: investigation of P-glycoprotein as a novel therapeutic target for Alzheimer's disease. *J Pharm Pharmacol* **63**: 1111-1118.

Abuznait AH and Kaddoumi A (2012) Role of ABC Transporters in the Pathogenesis of Alzheimer's Disease. *ACS Chem Neurosci* **3**: 820-831.

Annaert PP and Brouwer KL (2005) Assessment of drug interactions in hepatobiliary transport using rhodamine 123 in sandwich-cultured rat hepatocytes. *Drug Metab Dispos* **33**: 388-394.

Banks WA, Robinson SM, Verma S and Morley JE (2003) Efflux of human and mouse amyloid beta proteins 1-40 and 1-42 from brain: impairment in a mouse model of Alzheimer's disease. *Neuroscience* **121**: 487-492.

Bansal T, Mishra G, Jaggi M, Khar RK and Talegaonkar S (2009) Effect of P-glycoprotein inhibitor, verapamil, on oral bioavailability and pharmacokinetics of irinotecan in rats. *Eur J Pharm Sci* **36**: 580-590.

Bell RD, Sagare AP, Friedman AE, Bedi GS, Holtzman DM, Deane R and Zlokovic BV (2007) Transport pathways for clearance of human Alzheimer's amyloid beta-peptide and apolipoproteins E and J in the mouse central nervous system. *J Cereb Blood Flow Metab* **27**: 909-918.

Cam JA and Bu G (2006) Modulation of beta-amyloid precursor protein trafficking and processing by the low density lipoprotein receptor family. *Mol Neurodegener* **1**: 8.

Castellano JM, Deane R, Gottesdiener AJ, Verghese PB, Stewart FR, West T, Paoletti AC, Kasper TR, DeMattos RB, Zlokovic BV and Holtzman DM (2012) Low-density lipoprotein receptor overexpression enhances the rate of brain-to-blood Abeta clearance in a mouse model of beta-amyloidosis. *Proc Natl Acad Sci U S A* **109**: 15502-15507.

Chiang PK, Lam MA and Luo Y (2008) The many faces of amyloid beta in Alzheimer's disease. *Curr Mol Med* **8**: 580-584.

Cirrito JR, Deane R, Fagan AM, Spinner ML, Parsadanian M, Finn MB, Jiang H, Prior JL, Sagare A, Bales KR, Paul SM, Zlokovic BV, Piwnica-Worms D and Holtzman DM (2005) P-glycoprotein deficiency at the blood-brain barrier increases amyloid-beta deposition in an Alzheimer disease mouse model. *J Clin Invest* **115**: 3285-3290.

Deane R, Du Yan S, Submamaryan RK, LaRue B, Jovanovic S, Hogg E, Welch D, Manness L, Lin C, Yu J, Zhu H, Ghiso J, Frangione B, Stern A, Schmidt AM, Armstrong DL, Arnold B, Liliensiek B, Nawroth P, Hofman F, Kindy M, Stern D and Zlokovic B (2003) RAGE mediates amyloid-beta peptide transport across the blood-brain barrier and accumulation in brain. *Nat Med* **9**: 907-913.

Deane R, Sagare A and Zlokovic BV (2008) The role of the cell surface LRP and soluble LRP in blood-brain barrier Abeta clearance in Alzheimer's disease. *Curr Pharm Des* **14**: 1601-1605.

Deane R, Singh I, Sagare AP, Bell RD, Ross NT, LaRue B, Love R, Perry S, Paquette N, Deane RJ, Thiyagarajan M, Zarcone T, Fritz G, Friedman AE, Miller BL and Zlokovic BV (2012) A multimodal RAGE-specific inhibitor reduces amyloid beta-mediated brain disorder in a mouse model of Alzheimer disease. *J Clin Invest* **122**: 1377-1392.

Deane R, Wu Z, Sagare A, Davis J, Du Yan S, Hamm K, Xu F, Parisi M, LaRue B, Hu HW, Spijkers P, Guo H, Song X, Lenting PJ, Van Nostrand WE and Zlokovic BV (2004) LRP/amyloid beta-peptide interaction mediates differential brain efflux of Abeta isoforms. *Neuron* **43**: 333-344.

Donahue JE, Flaherty SL, Johanson CE, Duncan JA, 3rd, Silverberg GD, Miller MC, Tavares R, Yang W, Wu Q, Sabo E, Hovanesian V and Stopa EG (2006) RAGE, LRP-1, and amyloid-beta protein in Alzheimer's disease. *Acta Neuropathol* **112**: 405-415.

Eckman EA and Eckman CB (2005) Abeta-degrading enzymes: modulators of Alzheimer's disease pathogenesis and targets for therapeutic intervention. *Biochem Soc Trans* **33**: 1101-1105.

Ghiso J, Shayo M, Calero M, Ng D, Tomidokoro Y, Gandy S, Rostagno A and Frangione B (2004) Systemic catabolism of Alzheimer's Abeta40 and Abeta42. *J Biol Chem* **279**: 45897-45908.

Hardy J (2006) A hundred years of Alzheimer's disease research. *Neuron* **52**: 3-13.

Hartz AM, Miller DS and Bauer B (2010) Restoring blood-brain barrier P-glycoprotein reduces brain amyloid-beta in a mouse model of Alzheimer's disease. *Mol Pharmacol* **77**: 715-723.

Hewitt NJ, Lechon MJ, Houston JB, Hallifax D, Brown HS, Maurel P, Kenna JG, Gustavsson L, Lohmann C, Skonberg C, Guillouzo A, Tuschl G, Li AP, LeCluyse E, Groothuis GM and Hengstler JG (2007) Primary hepatocytes: current understanding of the regulation of metabolic enzymes and transporter proteins, and pharmaceutical practice for the use of hepatocytes in metabolism, enzyme induction, transporter, clearance, and hepatotoxicity studies. *Drug Metab Rev* **39**: 159-234.

Ito S, Ohtsuki S and Terasaki T (2006) Functional characterization of the brain-to-blood efflux clearance of human amyloid-beta peptide (1-40) across the rat blood-brain barrier. *Neurosci Res* **56**: 246-252.

Kuhnke D, Jedlitschky G, Grube M, Krohn M, Jucker M, Mosyagin I, Cascorbi I, Walker LC, Kroemer HK, Warzok RW and Vogelgesang S (2007) MDR1-P-Glycoprotein (ABCB1) Mediates Transport of Alzheimer's amyloid-beta peptides--implications for the mechanisms of Abeta clearance at the blood-brain barrier. *Brain Pathol* **17**: 347-353.

Lam FC, Liu R, Lu P, Shapiro AB, Renoir JM, Sharom FJ and Reiner PB (2001) beta-Amyloid efflux mediated by p-glycoprotein. *J Neurochem* **76**: 1121-1128.

Liu X, Chism JP, LeCluyse EL, Brouwer KR and Brouwer KL (1999a) Correlation of biliary excretion in sandwich-cultured rat hepatocytes and in vivo in rats. *Drug Metab Dispos* **27**: 637-644.

Liu X, LeCluyse EL, Brouwer KR, Gan LS, Lemasters JJ, Stieger B, Meier PJ and Brouwer KL (1999b) Biliary excretion in primary rat hepatocytes cultured in a collagen-sandwich configuration. *Am J Physiol* **277**: G12-21.

Mackic JB, Weiss MH, Miao W, Kirkman E, Ghiso J, Calero M, Bading J, Frangione B and Zlokovic BV (1998) Cerebrovascular accumulation and increased blood-brain barrier permeability to circulating Alzheimer's amyloid beta peptide in aged squirrel monkey with cerebral amyloid angiopathy. *J Neurochem* **70**: 210-215.

Makarova A, Williams SE and Strickland DK (2004) Proteases and lipoprotein receptors in Alzheimer's disease. *Cell Biochem Biophys* **41**: 139-178.

Marques MA, Kulstad JJ, Savard CE, Green PS, Lee SP, Craft S, Watson GS and Cook DG (2009) Peripheral amyloid-beta levels regulate amyloid-beta clearance from the central nervous system. *J Alzheimers Dis* **16**: 325-329.

Pflanzner T, Janko MC, Andre-Dohmen B, Reuss S, Weggen S, Roebroek AJ, Kuhlmann CR and Pietrzik CU (2011) LRP1 mediates bidirectional transcytosis of amyloid-beta across the blood-brain barrier. *Neurobiol Aging* **32**: 2323 e2321-2311.

Qosa H, Abuznait AH, Hill RA and Kaddoumi A (2012) Enhanced brain amyloid-beta clearance by rifampicin and caffeine as a possible protective mechanism against Alzheimer's disease. *J Alzheimers Dis* **31**: 151-165.

Quinn KA, Grimsley PG, Dai YP, Tapner M, Chesterman CN and Owensby DA (1997) Soluble low density lipoprotein receptor-related protein (LRP) circulates in human plasma. *J Biol Chem* **272**: 23946-23951.

Sagare A, Deane R, Bell RD, Johnson B, Hamm K, Pendu R, Marky A, Lenting PJ, Wu Z, Zarcone T, Goate A, Mayo K, Perlmutter D, Coma M, Zhong Z and Zlokovic BV (2007) Clearance of amyloid-beta by circulating lipoprotein receptors. *Nat Med* **13**: 1029-1031.

Sagare AP, Bell RD and Zlokovic BV (2012) Neurovascular dysfunction and faulty amyloid beta-peptide clearance in Alzheimer disease. *Cold Spring Harb Perspect Med* **2**. : a011452.

Sagare AP, Deane R, Zetterberg H, Wallin A, Blennow K and Zlokovic BV (2011) Impaired lipoprotein receptor-mediated peripheral binding of plasma amyloid-beta is an early biomarker for mild cognitive impairment preceding Alzheimer's disease. *J Alzheimers Dis* **24**: 25-34.

Saido T and Leissring MA (2012) Proteolytic Degradation of Amyloid beta-Protein. *Cold Spring Harb Perspect Med* **2**: a006379.

Seeman P and Seeman N (2011) Alzheimer's disease: beta-amyloid plaque formation in human brain. *Synapse* **65**: 1289-1297.

Seglen PO (1976) Preparation of isolated rat liver cells. *Methods Cell Biol* **13**: 29-83.

Sehgal N, Gupta A, Valli RK, Joshi SD, Mills JT, Hamel E, Khanna P, Jain SC, Thakur SS and Ravindranath V (2012) Withania somnifera reverses Alzheimer's disease pathology by enhancing low-density lipoprotein receptor-related protein in liver. *Proc Natl Acad Sci U S A* **109**: 3510-3515.

Shibata M, Yamada S, Kumar SR, Calero M, Bading J, Frangione B, Holtzman DM, Miller CA, Strickland DK, Ghiso J and Zlokovic BV (2000) Clearance of Alzheimer's amyloid-ss(1-40) peptide from brain by LDL receptor-related protein-1 at the blood-brain barrier. *J Clin Invest* **106**: 1489-1499.

Silverberg GD, Messier AA, Miller MC, Machan JT, Majmudar SS, Stopa EG, Donahue JE and Johanson CE (2010) Amyloid efflux transporter expression at the blood-brain barrier declines in normal aging. *J Neuropathol Exp Neurol* **69**: 1034-1043.

Sommer B (2002) Alzheimer's disease and the amyloid cascade hypothesis: ten years on. *Curr Opin Pharmacol* **2**: 87-92.

Sugimoto H, Matsumoto S, Tachibana M, Niwa S, Hirabayashi H, Amano N and Moriwaki T (2011) Establishment of in vitro P-glycoprotein inhibition assay and its exclusion criteria to assess the risk of drug-drug interaction at the drug discovery stage. *J Pharm Sci* **100**: 4013-4023.

Sutcliffe JG, Hedlund PB, Thomas EA, Bloom FE and Hilbush BS (2011) Peripheral reduction of beta-amyloid is sufficient to reduce brain beta-amyloid: implications for Alzheimer's disease. *J Neurosci Res* **89**: 808-814.

Swift B, Pfeifer ND and Brouwer KL (2010) Sandwich-cultured hepatocytes: an in vitro model to evaluate hepatobiliary transporter-based drug interactions and hepatotoxicity. *Drug Metab Rev* **42**: 446-471.

Sziraki I, Erdo F, Beery E, Molnar PM, Fazakas C, Wilhelm I, Makai I, Kis E, Heredi-Szabo K, Abonyi T, Krizbai I, Toth GK and Krajcsi P (2011) Quinidine as an ABCB1 probe for testing drug interactions at the blood-brain barrier: an in vitro in vivo correlation study. *J Biomol Screen* **16**: 886-894.

Tamaki C, Ohtsuki S, Iwatsubo T, Hashimoto T, Yamada K, Yabuki C and Terasaki T (2006) Major involvement of low-density lipoprotein receptor-related protein 1 in the clearance of plasma free amyloid beta-peptide by the liver. *Pharm Res* **23**: 1407-1416.

Tamaki C, Ohtsuki S and Terasaki T (2007) Insulin facilitates the hepatic clearance of plasma amyloid beta-peptide (1 40) by intracellular translocation of low-density lipoprotein receptor-related protein 1 (LRP-1) to the plasma membrane in hepatocytes. *Mol Pharmacol* **72**: 850-855.

Toornvliet R, van Berckel BN, Luurtsema G, Lubberink M, Geldof AA, Bosch TM, Oerlemans R, Lammertsma AA and Franssen EJ (2006) Effect of age on functional P-glycoprotein in the blood-brain barrier measured by use of (R)-[(11)C]verapamil and positron emission tomography. *Clin Pharmacol Ther* **79**: 540-548.

Turncliff RZ, Tian X and Brouwer KL (2006) Effect of culture conditions on the expression and function of Bsep, Mrp2, and Mdr1a/b in sandwich-cultured rat hepatocytes. *Biochem Pharmacol* **71**: 1520-1529.

Vogelgesang S, Cascorbi I, Schroeder E, Pahnke J, Kroemer HK, Siegmund W, Kunert-Keil C, Walker LC and Warzok RW (2002) Deposition of Alzheimer's beta-amyloid is inversely correlated with P-glycoprotein expression in the brains of elderly non-demented humans. *Pharmacogenetics* **12**: 535-541.

Zhao LN, Long H, Mu Y and Chew LY (2012) The Toxicity of Amyloid beta Oligomers. *Int J Mol Sci* **13**: 7303-7327.

Zlokovic BV, Yamada S, Holtzman D, Ghiso J and Frangione B (2000) Clearance of amyloid beta-peptide from brain: transport or metabolism? *Nat Med* **6**: 718-719.

Figures Legend

Figure 1: Phase-contrast image of SCHs cultured for 4 days with formed canalicular spaces as indicated by the white arrows (A), and fluorescence micrograph of SCHs at day 4 of culture after pretreatment with 2µM CDFDA dissolved in standard HBSS which was metabolized and effluxed rapidly into the canalicular spaces showed as intense green fluorescent as indicated by the arrows (B).

Figure 2: Western blot analysis of P-gp, LRP1, and RAGE protein expression in SCHs at day 4 of culture with or without 48 h treatment with 50 µM rifampicin started from day 2 of sandwich cultured hepatocytes (A), with their corresponding densitometry analysis (B). Bars represent mean ± SEM of n = 3; ** P<0.01, *** P<0.001, and ns is not significant.

Figure 3: (A) Cumulative uptake of 1µM [^{14}C] salicylic acid ([^{14}C] SA), and 1µM [^{3}H] taurocholate ([^{3}H] TC) in SCHs at day 4 of culture. Hepatocytes were preincubated for 10 min in standard HBSS or Ca^{++}-free HBSS before cumulative uptake studies were conducted. BEI% and Cl_{bile} (ml/min/kg of animal) were determined after 10 min of addition of [^{14}C] SA and [^{3}H] TC. Each bar represents the mean±SEM for four replicates from three independent experiments. *** P<0.001, and ns = not significant, between substrates cumulative uptake from standard HBSS and Ca^{++}-free HBSS based on unpaired student *t* test. (B) Cumulative efflux of Rh123 into standard HBSS and Ca^{++}-free HBSS for 30 min in SCHs at day 4 of culture. Hepatocytes were preloaded with 1µM Rh123 dissolved in standard HBSS for 30 min at 37^{o}C followed by efflux study. Bars represents mean±SEM for triplicates from two independent experiments. Unpaired

student *t* test was used to compare between Rh123 efflux into standard and Ca^{++}-free HBSS, * $P<0.05$.

Figure 4: Representative time course of $^{125}I\text{-}A\beta_{40}$ biliary excretion index (BEI%) in SCHs at day 4. Cumulative uptake of 0.14 nM $^{125}I\text{-}A\beta_{40}$ dissolved in standard or Ca^{++}-free HBSS for 5, 15, 30 and 60 min were determined and BEI% was calculated at each time point. Points represent BEI% of $A\beta_{40}$ for n = 4, * $P<0.05$ compared to 5 and 15 min, ns = not significant compared to 30 min based on unpaired Student's *t* test.

Figure 5: (A) Cumulative uptake of 0.14 nM $^{125}I\text{-}A\beta_{40}$ in standard and Ca^{++}-free HBSS after 5 and 30 min incubation in hepatocyte conventional culture and hepatocytes cultured in sandwich configuration for 2 days. (B) Cumulative uptake of 0.14 nM $^{125}I\text{-}A\beta_{40}$ in standard and Ca^{++}-free HBSS in SCHs for 30 min at days 2 and 4 of culture. Aliquots were taken from cells lysate incubated with or without calcium, and degraded $^{125}I\text{-}A\beta_{40}$ was determined using TCA assay. Bars represent the mean ± SEM (n = 4), * $P<0.05$ and ** $P<0.01$ compared to corresponding control.

Figure 6: Cumulative uptake, BEI% and Cl_{bile} of 0.14 nM $^{125}I\text{-}A\beta_{40}$ with or without P-gp specific inhibitors verapamil (50μM) and valspodar (20μM). BEI% and Cl_{bile} were determined at 30 min in SCHs, day 4 of culture. Bars represent the mean ± SEM (n = 4), * $P<0.05$ and *** $P<0.001$ for verapamil and valspodar treated cells, grey bars (Ca^{++}-free HBSS), compared to corresponding control.

DMD Fast Forward. Published on July 12, 2013 as DOI: 10.1124/dmd.113.052514
This article has not been copyedited and formatted. The final version may differ from this version.

Figure 7: Cumulative uptake, BEI% and Cl_{bile} of 0.14 nM ^{125}I-Aβ_{40} with or without LRP1 and RAGE specific inhibitors; RAP (1 µM) and RAGE-IgG antibody (10 µg/ml), respectively. BEI% and Cl_{bile} (ml/min/kg body weight) were determined at 30 min in SCHs, day 4 of culture. Bars represent the mean ± SEM (n = 4), * $P<0.05$ for RAP and RAGE-IgG treated groups, black bars (Ca^{++}- HBSS), compared to corresponding control.

Figure 8: Immunofluorescence localization of RAGE in SCHs cultured for 4 days. Hepatocyte culture was viewed with fluorescence merged with phase contrast and DAPI for nuclei staining. Culture labeled with specific RAGE monoclonal antibody followed by FITC-conjugated secondary antibody showed absence of signal at canaliculi (white arrows) and presence of green fluorescence at the sinusoidal front.

Figure 9: BEI% of ^{125}I-Aβ_{40} with or without P-gp specific inhibitor, verapamil (50 µM), in rifampicin (50 µM) or vehicle treated cells. BEI% was determined at 30 min in SCHs, day 4 of culture. Bars represent the mean ± SEM (n = 3), * $P<0.05$, ** $P<0.01$ and *** $P<0.001$.

Figure 1

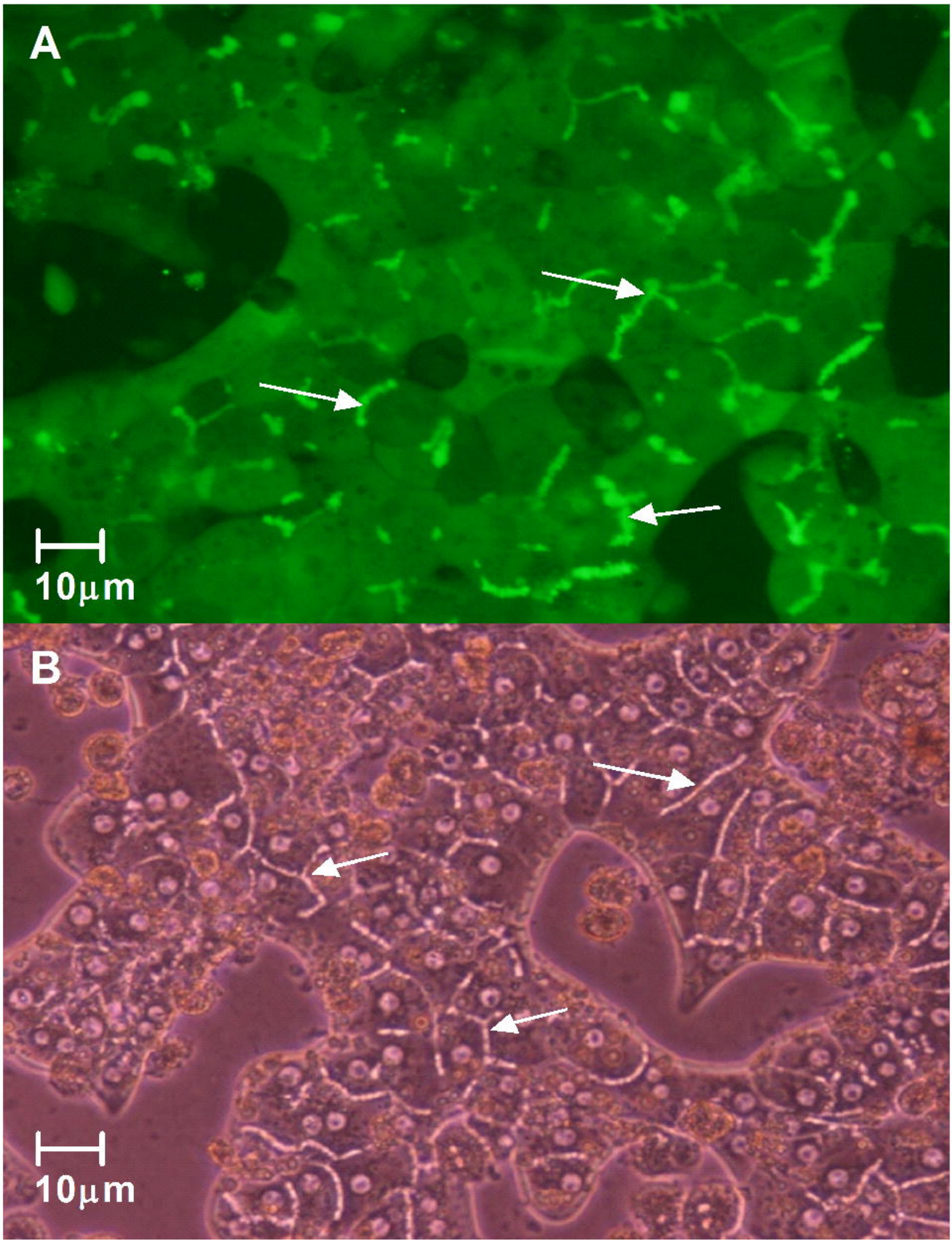

Figure 2

A

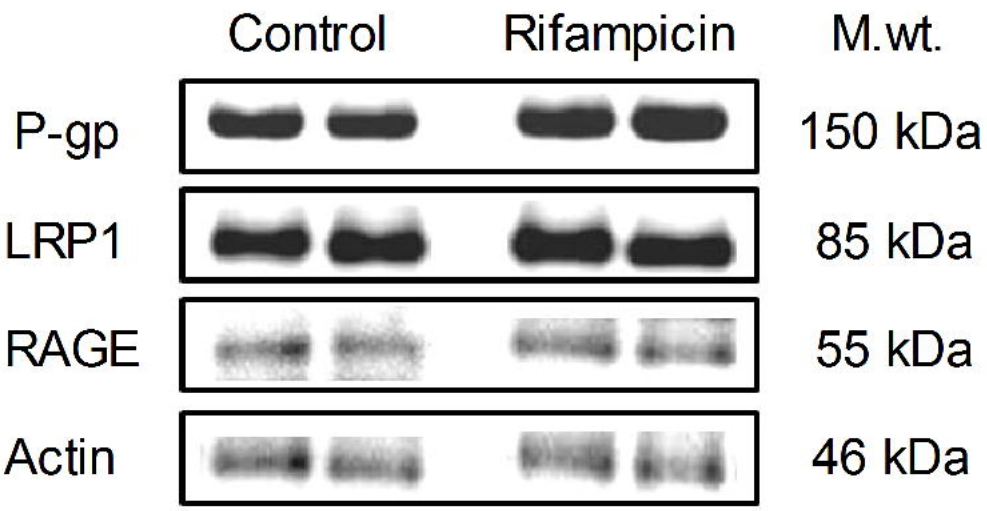
Control
Rifampicin
M.wt.
P-gp
150 kDa
LRP1
85 kDa
RAGE
55 kDa
Actin
46 kDa

B

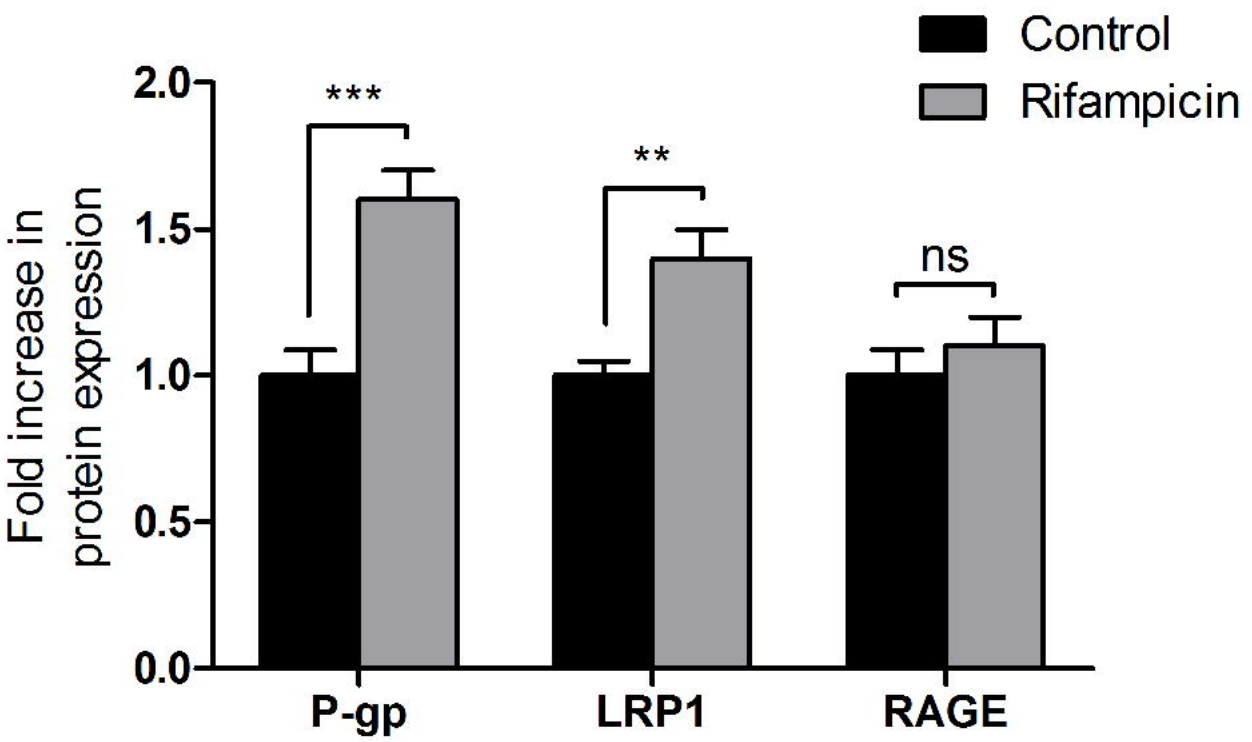
Control
Rifampicin
Fold increase in protein expression
2.0
1.5
1.0
0.5
0.0
***
**
ns
P-gp
LRP1
RAGE

Figure 3

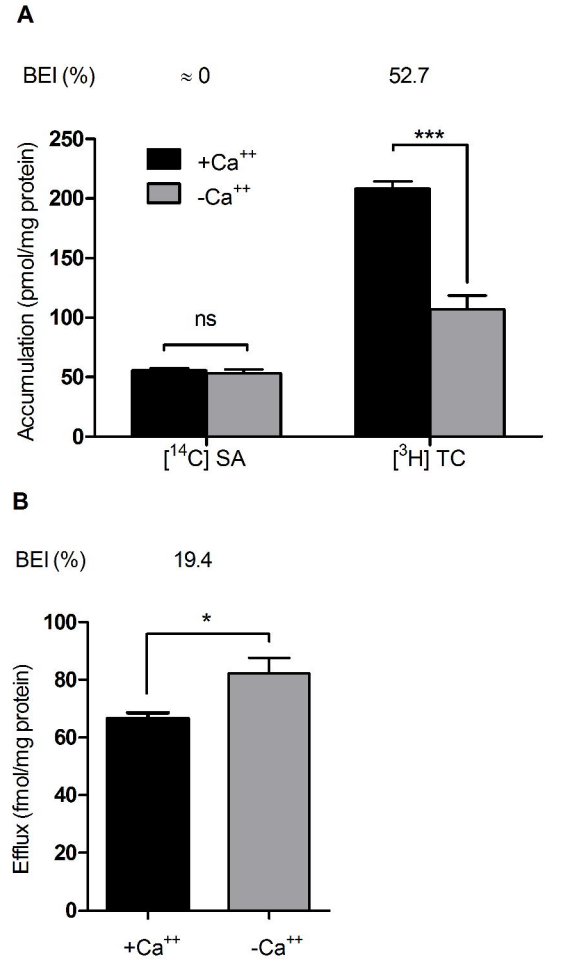
A
BEI (%)
≈ 0
52.7
250
200
150
100
50
0
Accumulation (pmol/mg protein)
+Ca++
-Ca++
***
ns
[14C] SA
[3H] TC
B
BEI (%)
19.4
100
80
60
40
20
0
Efflux (fmol/mg protein)
*
+Ca++
-Ca++

Figure 4

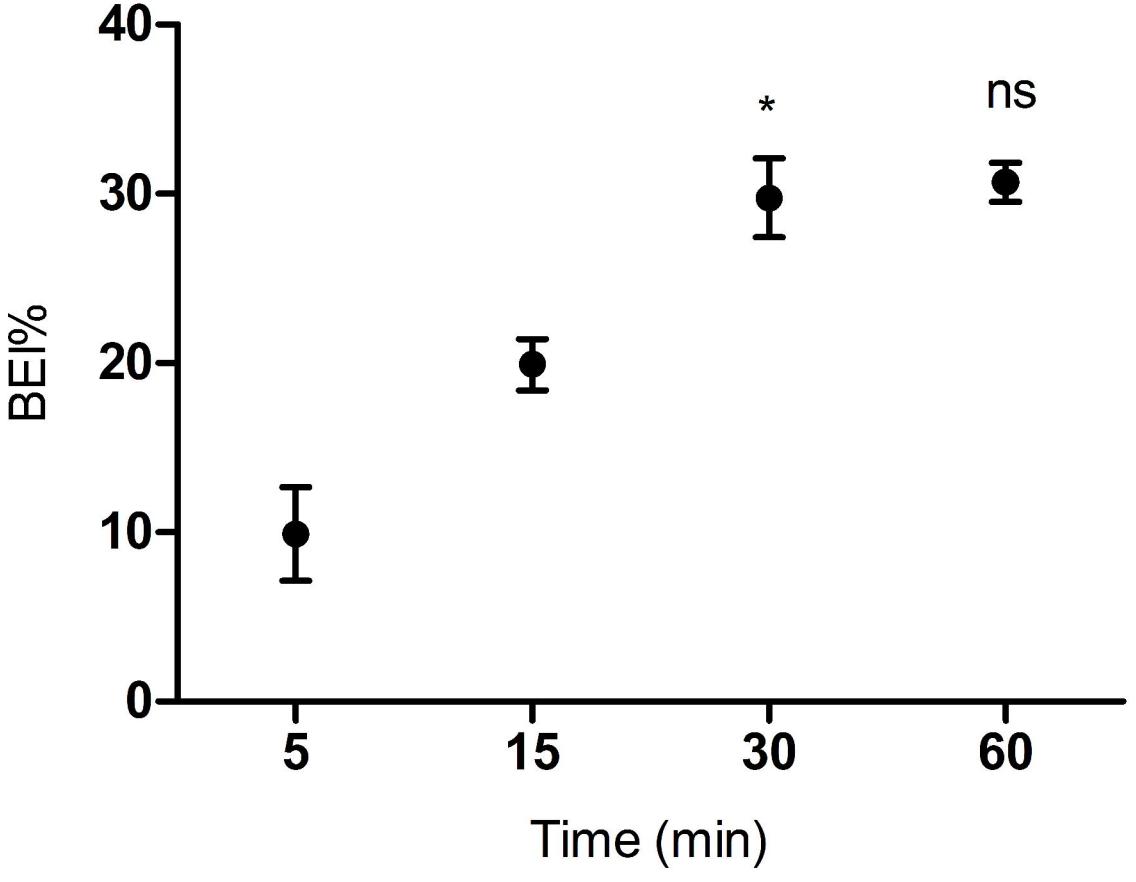

Figure 5

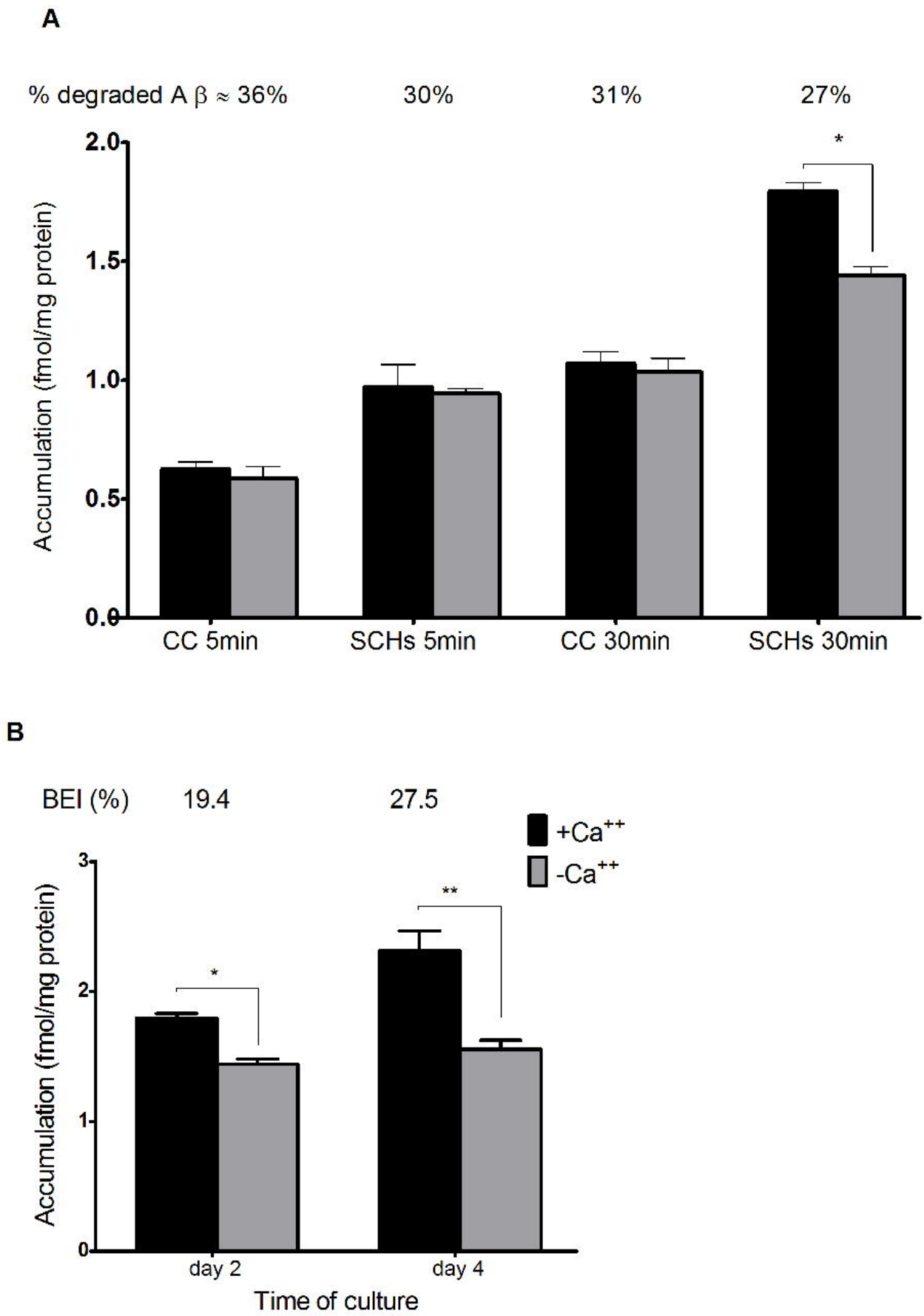
A
% degraded A β ≈ 36%
30%
31%
27%
2.0
1.5
1.0
0.5
0.0
Accumulation (fmol/mg protein)
*
CC 5min
SCHs 5min
CC 30min
SCHs 30min
B
BEI (%)
19.4
27.5
+Ca++
-Ca++
3
2
1
0
Accumulation (fmol/mg protein)
*
**
day 2
day 4
Time of culture

Figure 6

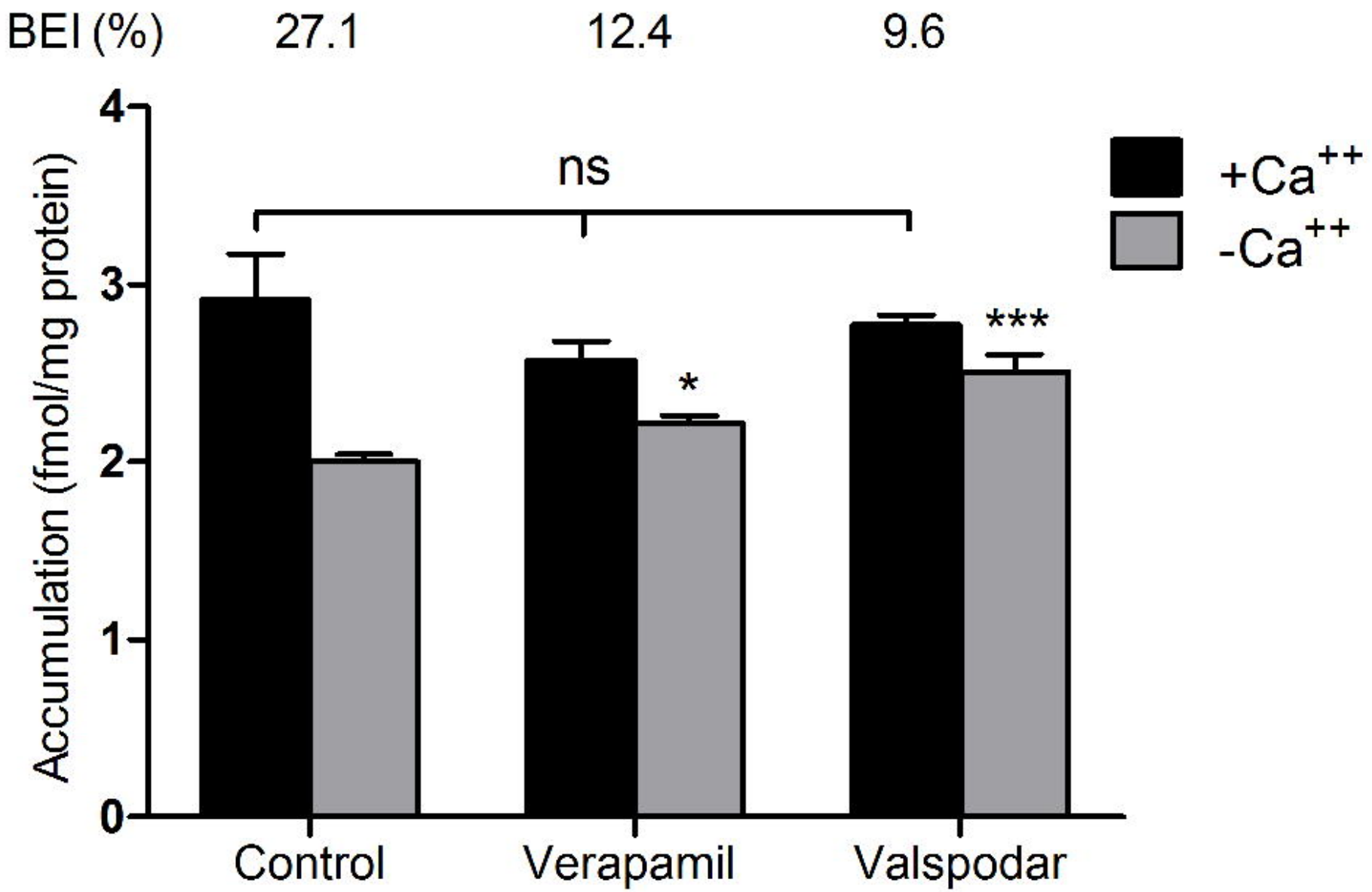
BEI (%)
27.1
12.4
9.6
Accumulation (fmol/mg protein)
4
3
2
1
0
ns
*
***
+Ca++
-Ca++
Control
Verapamil
Valspodar

Figure 7

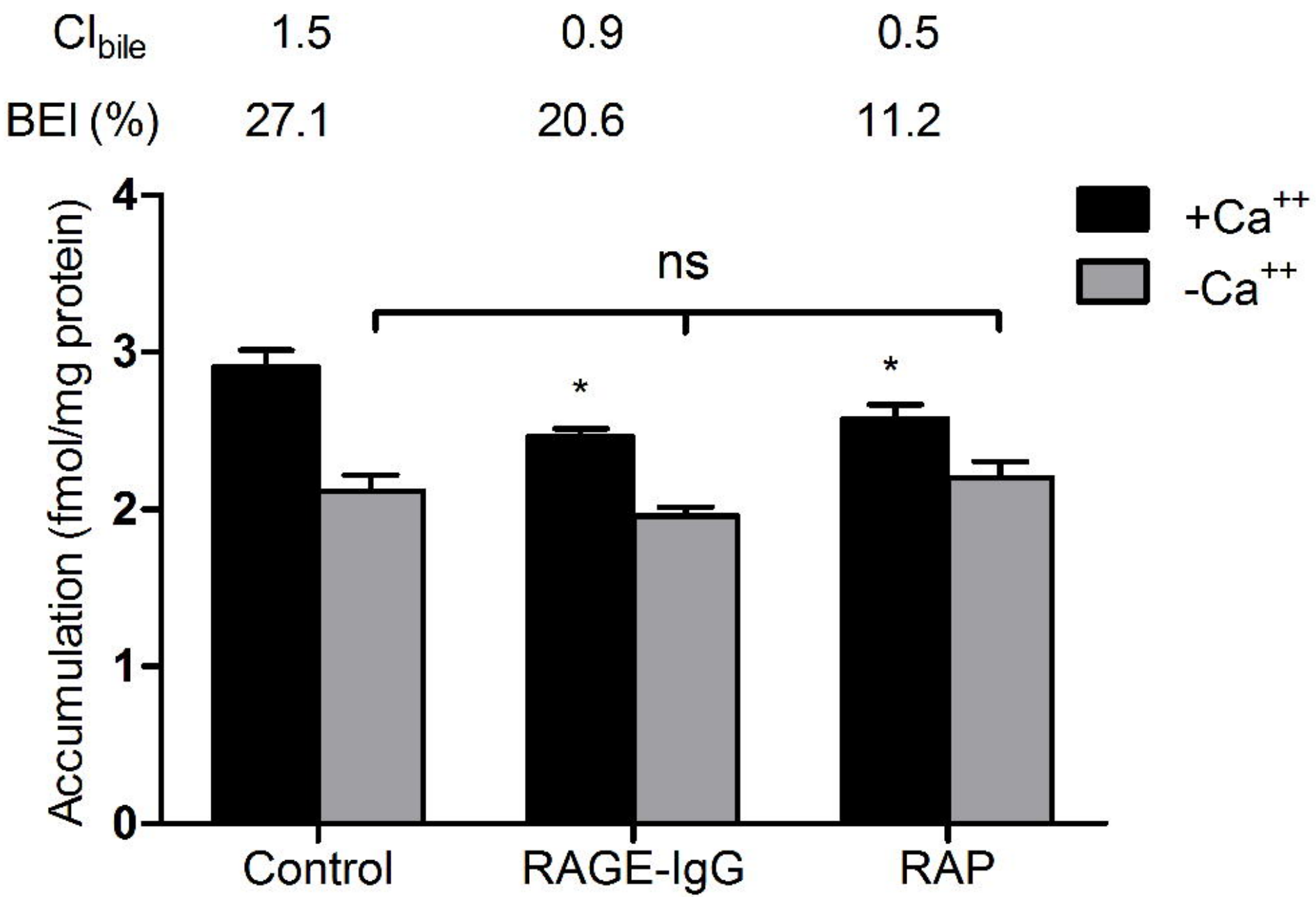
Cl_{bile} 1.5 0.9 0.5
BEI (%) 27.1 20.6 11.2
Accumulation (fmol/mg protein)
0
1
2
3
4
ns
*
*
+Ca++
-Ca++
Control
RAGE-IgG
RAP

Figure 8

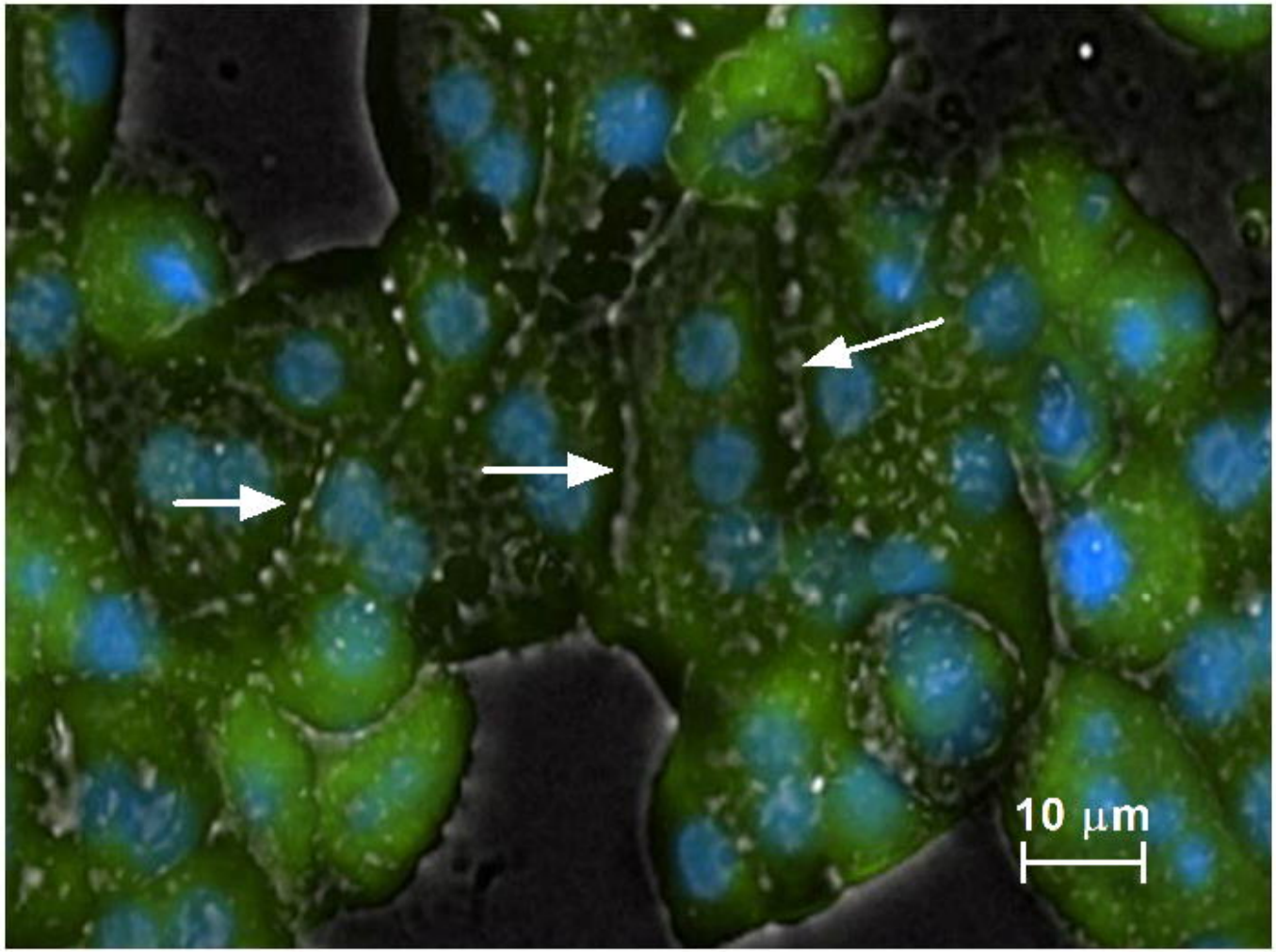

Figure 9

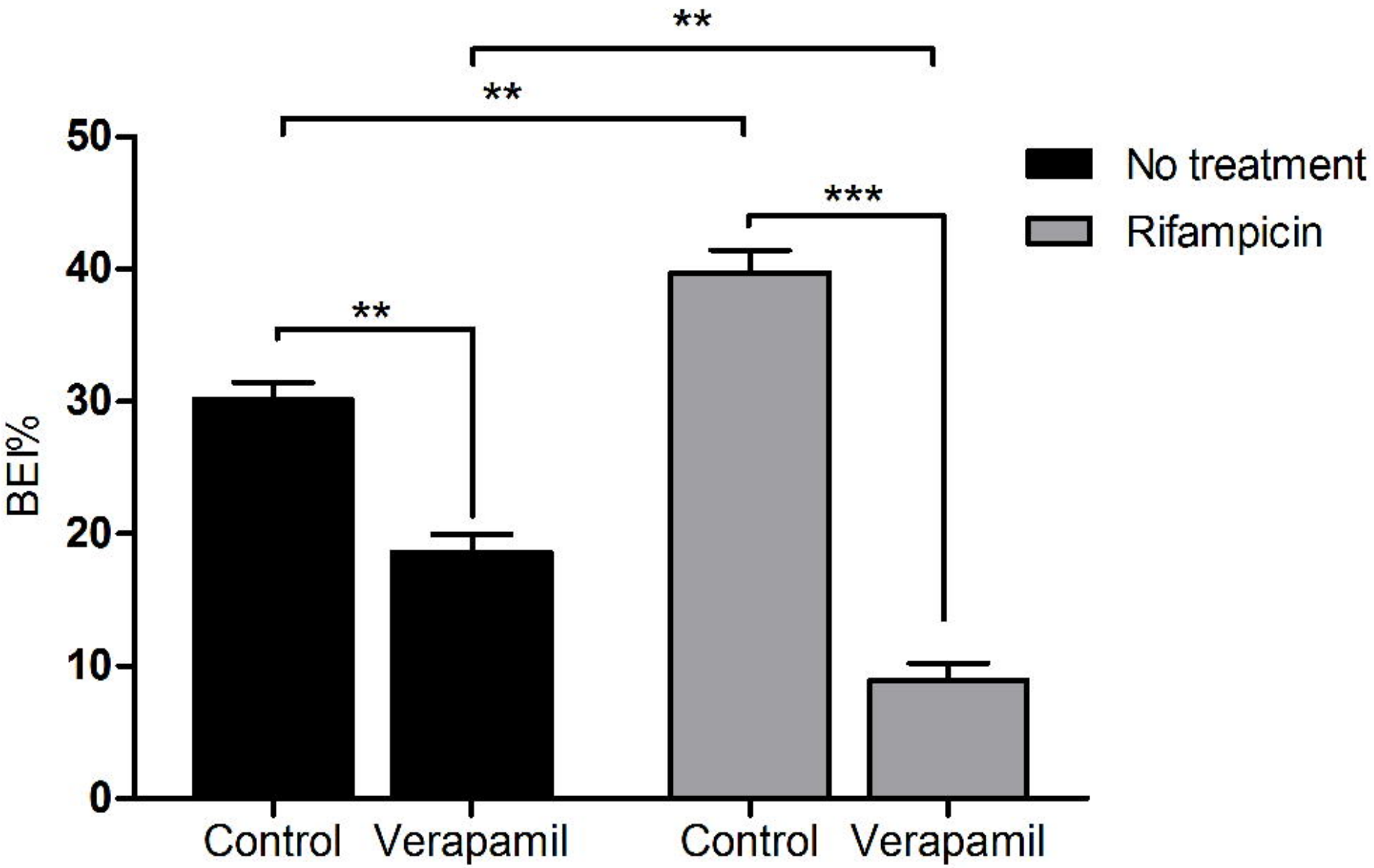
**
**
**
***
50
40
30
20
10
0
BEI%
No treatment
Rifampicin
Control
Verapamil
Control
Verapamil